Enhanced uptake in 2D- and 3D- lung cancer cell models of redox responsive PEGylated nanoparticles with sensitivity to reducing extra- and intracellular environments

Claudia Conte[1], Francesca Mastrotto[1,2], Vincenzo Taresco[1], Aleksandra Tchoryk[1], Fabiana Quaglia[3], Snjezana Stolnik[1], and Cameron Alexander[1*]

[1] Division of Molecular Therapeutics and Formulation, School of Pharmacy, University of Nottingham, UK, [2] Department of Pharmaceutical and Pharmacological Sciences, University of Padova, Padova, Italy, [3] Drug Delivery Laboratory, Department of Pharmacy, University of Napoli Federico II, Napoli, Italy. F. Mastrotto and V. Taresco contributed equally to this work.

[*]Corresponding author:

Prof. Cameron Alexander:

tel +44 (0) 115 846 7678

Supporting Information

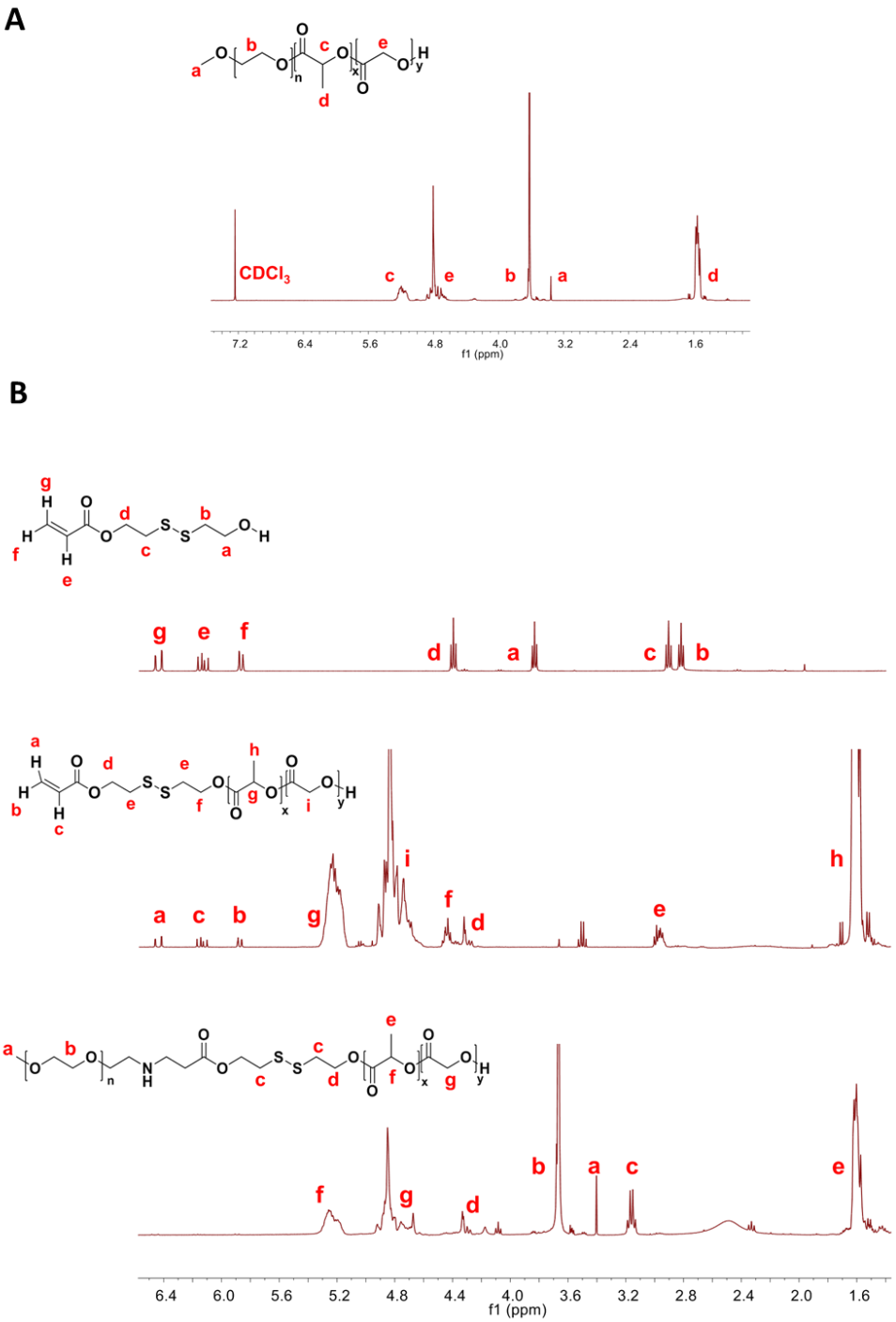

Figure S1: ^{1}H NMR spectra of PLGA-PEG (A) and PLGA-ss-PEG and intermediates (2-((hydroxymethyl)disulfanyl)ethyl acrylate and PLGA-SS) (B) in $CDCl_3$.

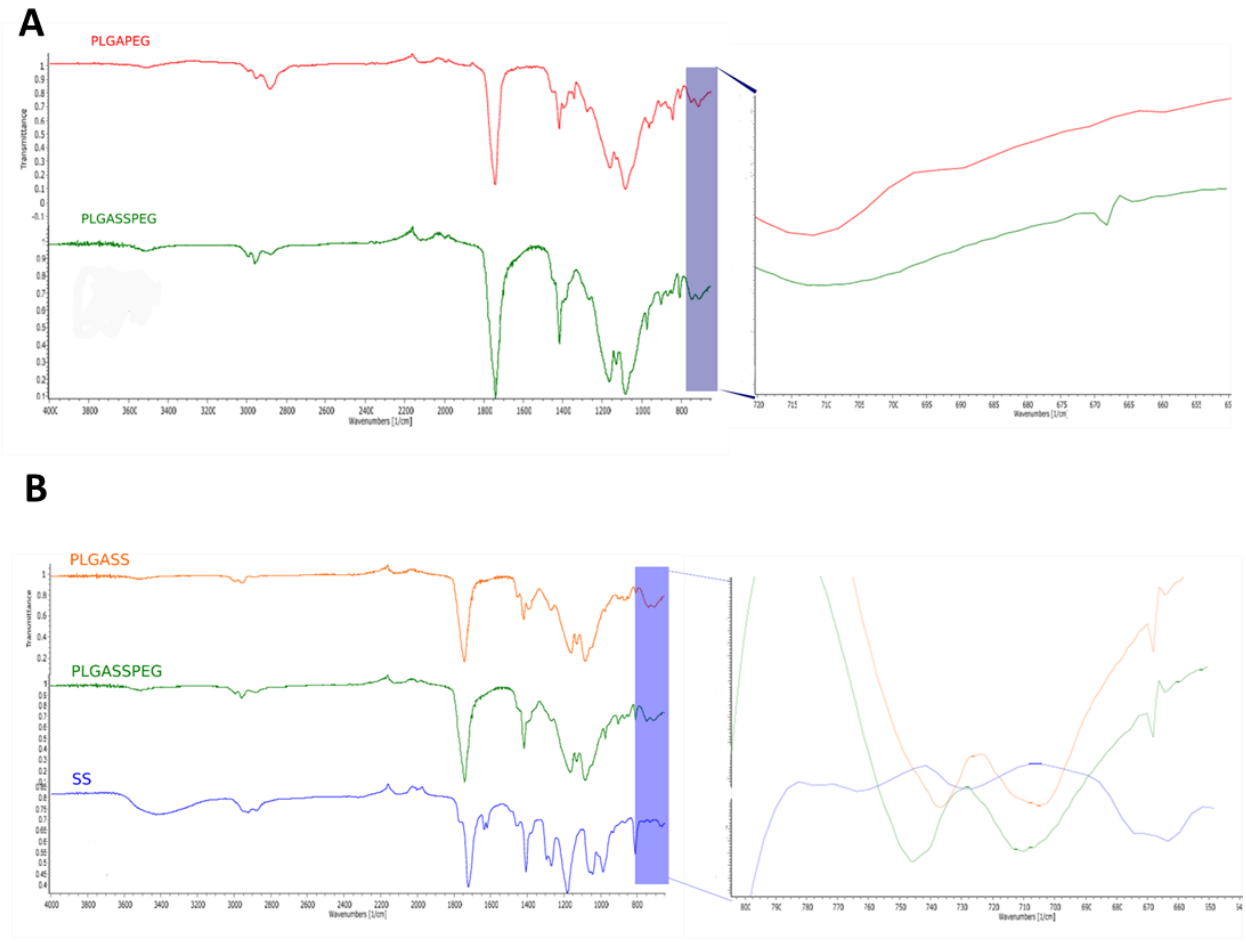

Figure S2. AT-IR spectra of A) PLGA-PEG vs PLGA-ss-PEG: a sharp peak at around 665 cm^{-1} 1725 cm^{-1} for the C-S stretching is evident in the inset; (B) PLGA-S-S-PEG and intermediates: in the inset, the C-S stretching mode at around 665 cm^{-1} is indicated for PLGA –S-S and PLGA-ss-PEG, whereas a broad, more pronounced peak is evident for 2-((hydroxymethyl)disulfanyl)ethyl acrylate

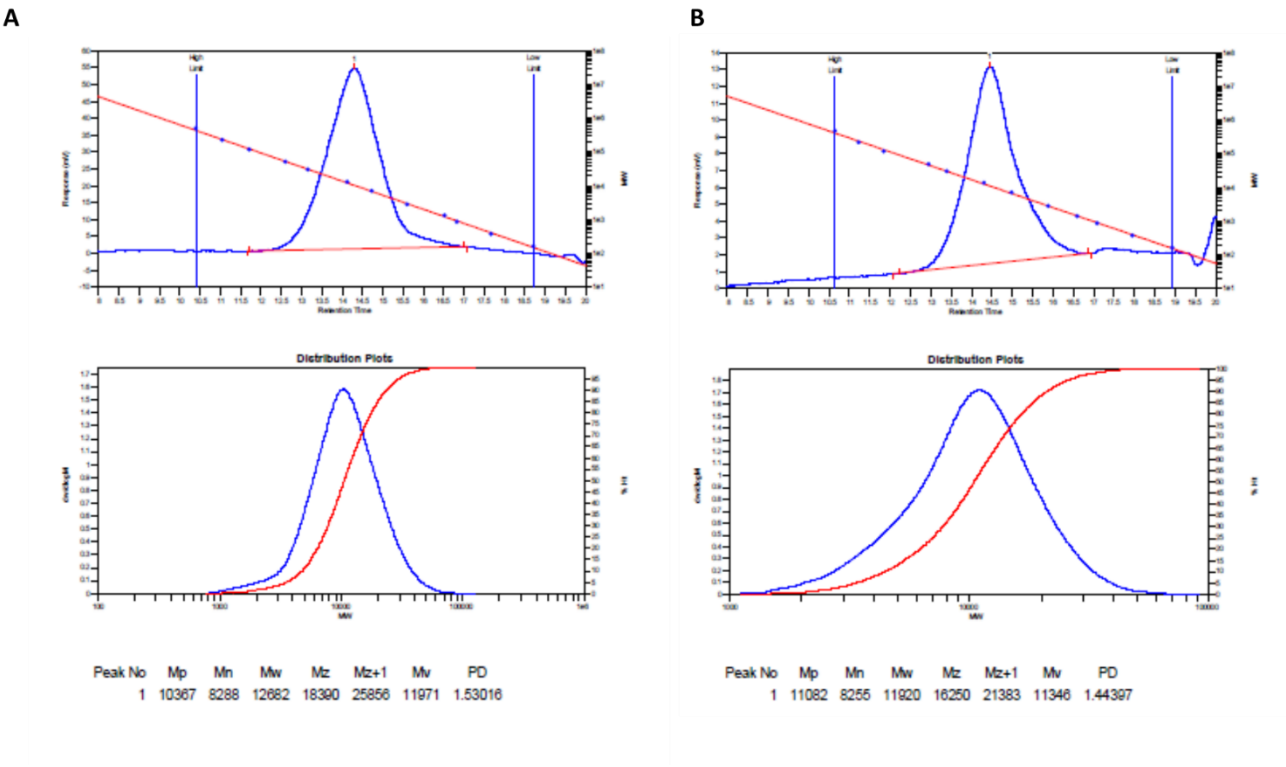

Figure S3: SEC traces of PLGA-PEG (A) and PLGA-ss-PEG (B) in CHCl3 (PS calibration).

Table S1. Thermal properties of homopolymer and copolymers

Polymer	Tg (°C)	Tm (°C)	DH(J/g)	Θ (contact angle)
PEG-NH_2	-	49.7	123.2	17.6
PLGA-PEG	-5.4	-	-	49.5
PLGA-SS	36.4	-	-	70.1
PLGA-ss-PEG	13.9	-	-	52.4

Table S2. Characterization of NPs loaded with different model drugs.

Code	Yield (%)	Mean D_H (nm ± SD)	P.I.	Zeta Potential (mV ± SD)
Rhod6G/nRR-NPs	80	147 ±4.5	0.190	-29.2±4.3
Fluo/nRR-NPs	85	154±8.2	0.184	-30.5±6.2
Rhod6G-Fluo/nRR-NPs	86	144 ±6.6	0.192	-31.7±3.2
DiO/nRR-NPs	89	142±3.3	0.212	-27.5±4.6
DiL/nRR-NPs	83	151±4.7	0.182	-28.7±2.3
DiO-DiL/nRR-NPs	88	154 ±8.5	0.167	-27.9±2.7
Rhod6G/RR-NPs	75	145±4.2	0.260	-28.5±3.3
Fluo/RR-NPs	73	141±3.7	0.198	-28.0±1.5
Rhod6G-Fluo/RR-NPs	70	133 ±4.2	0.184	-29.0±2.3
DiO/RR-NPs	75	154±2.5	0.172	-30.4±0.7
DiL/RR-NPs	71	148±4.8	0.183	-27.3±5.1
DiO-DiL/RR-NPs	74	139 ±7.2	0.176	-30.4±3.7

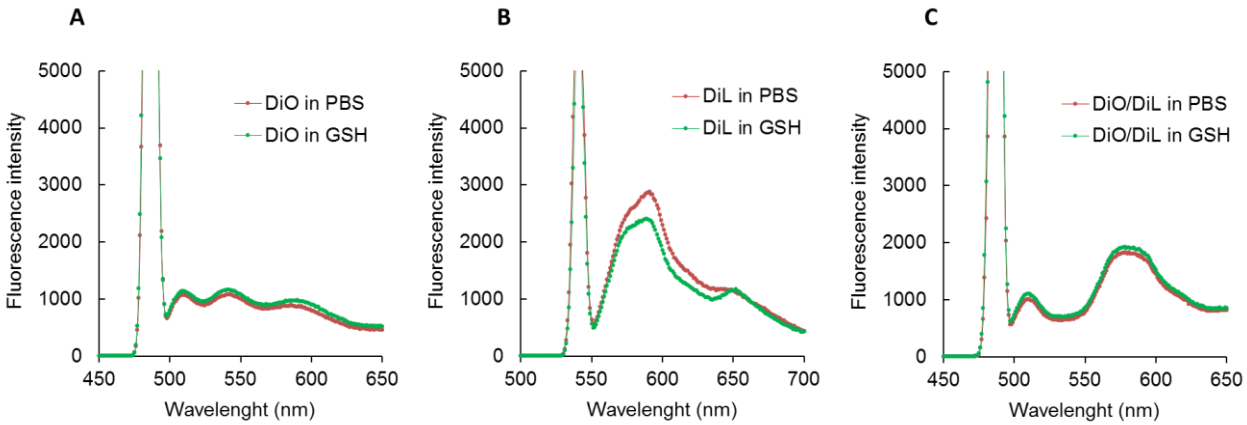

Figure S4: Fluorescence-emission spectra of free dyes alone and in combination dissolved in PBS 10 mM pH 7.4 with or without GSH 10 mM after 4h of incubation starting from stock solutions in EtOH. The concentration of the dyes was 0.6 μg/mL. A) DiO at λ_{ex}488, B) DiL at λ_{ex}543 and C) DiO/DiL mixture (FRET effect) at λ_{ex}488. The FRET efficiency ratio ($I_{575/505}$) of DiO/DiL in PBS and in GSH was not significantly different (1.81 and 1.89 respectively).

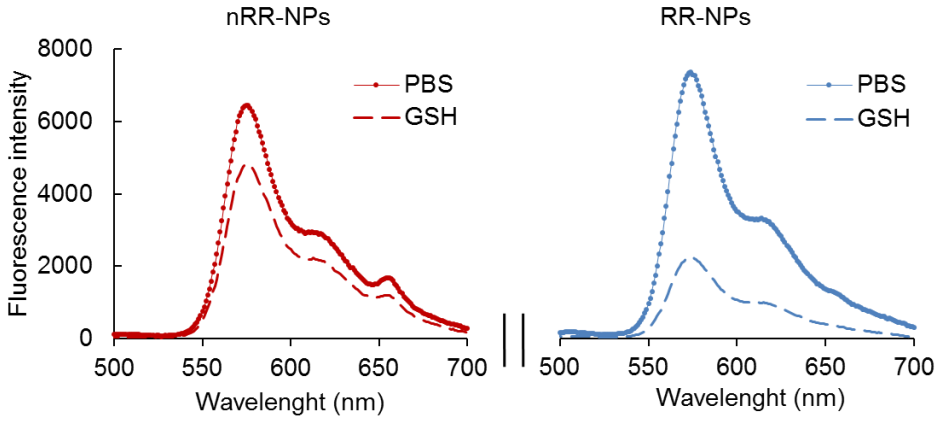

Figure S5: Fluorescence-emission spectra of FRET NPs (λex 488 nm) dispersed in PBS and penetrated through an artificial mucus layer (24h) with or without pre- treatment with GSH 10 mM.

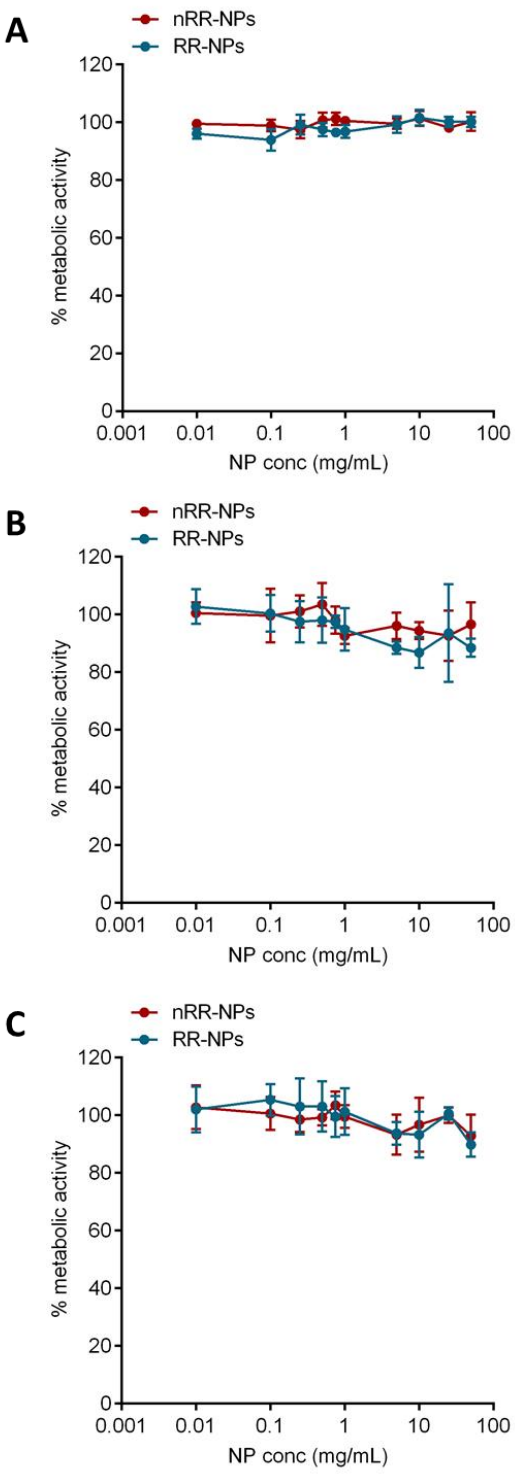

Figure S6. Cytotoxicity of unloaded NPs as measured by metabolic activity of A549 (A), H1299 (B) and Calu-3 (C) lung cancer cells after 24 h of treatment.

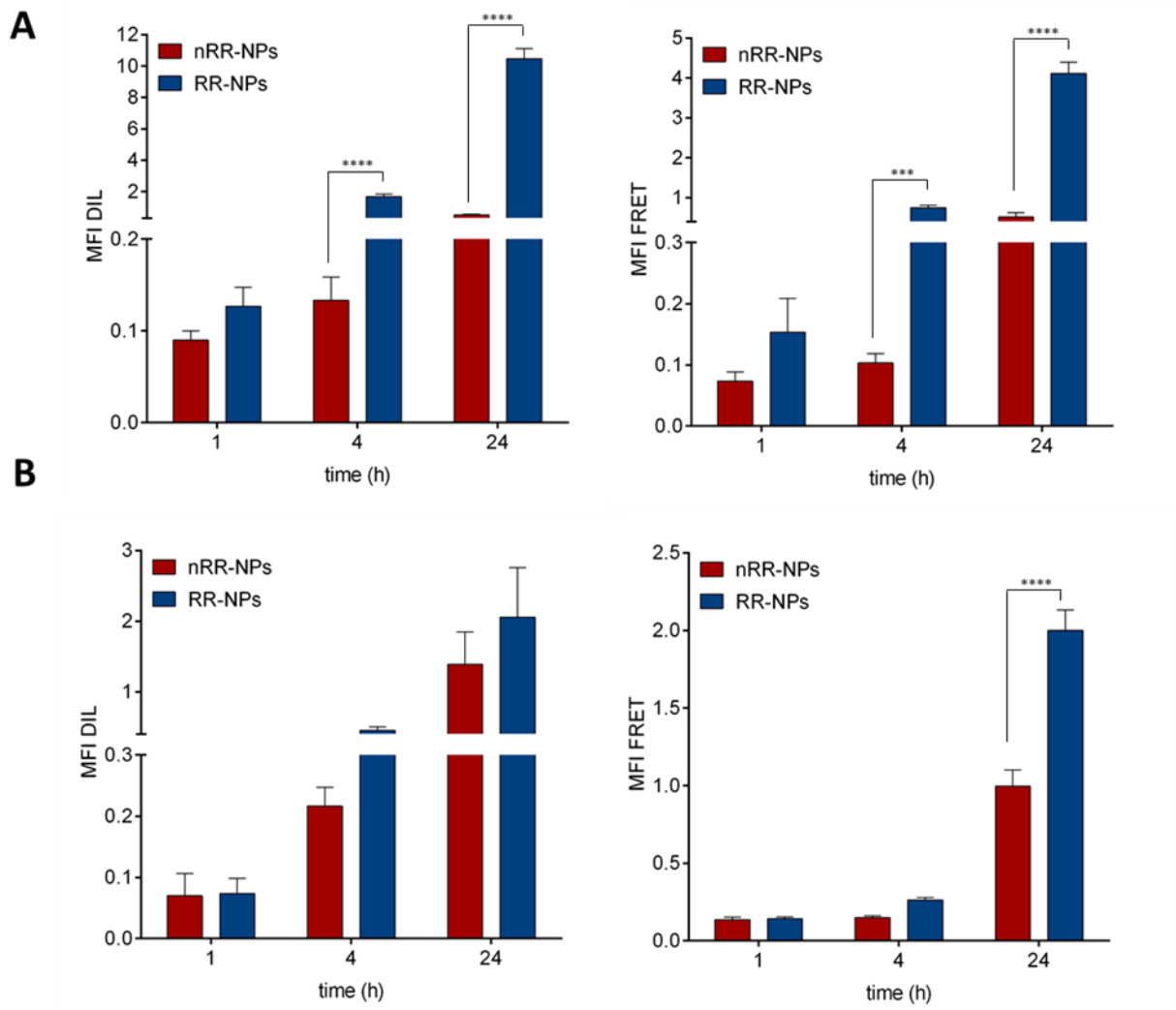

Figure S7. FACS measurements of DiL and FRET MFI of Calu-3 (A) and H1299 (B) cells treated with FRET NPs after 1h, 4h and 24h of incubation. ****P<0.0001, two-way ANOVA test

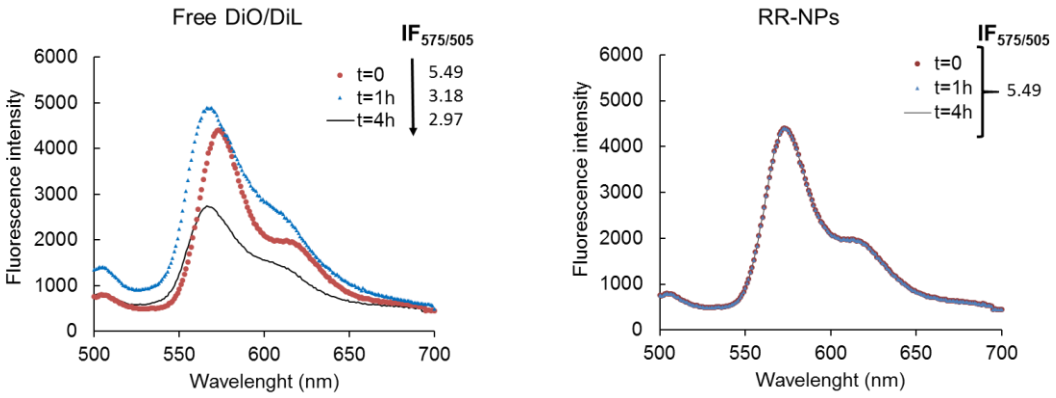

Figure S8. Time-resolved spectra of FRET RR-NPs (lex 488 nm) or free dyes dispersed in cell culture media in the presence of 2 mg/mL of SUV solution as cell membrane model. The concentration of the dyes in free solution or entrapped into NPs was 0.6 μg/mL to simulate the experimental conditions of cell studies.

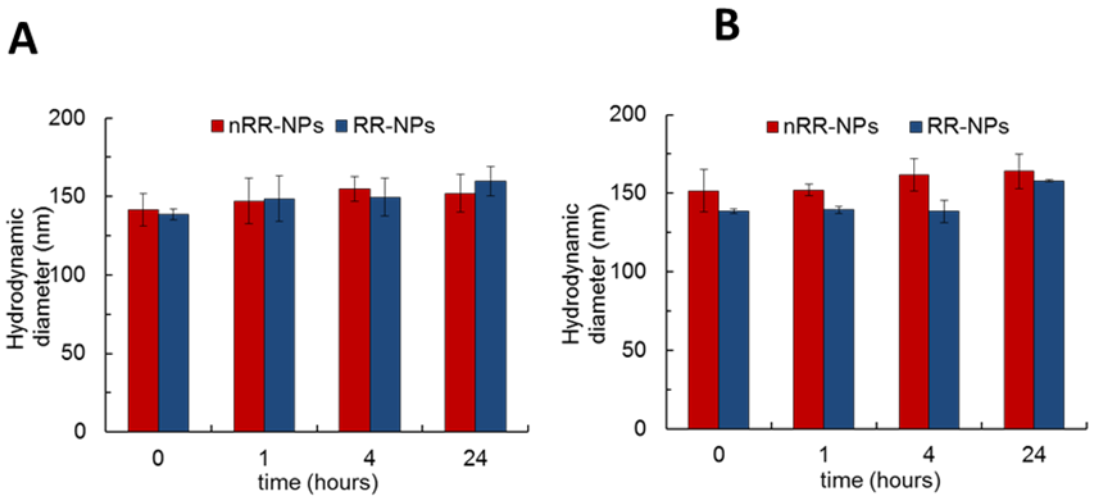

.

Figure S9. Stability of NPs in DMEM cell culture media with (A) or without B) FBS 10%.